ENVIRONMENTAL RESEARCH
LETTERS

LETTER • OPEN ACCESS

Skillful prediction of tropical Pacific fisheries provided by Atlantic Niños

IOP Publishing Environ. Res. Lett. 16 (2021) 054066 https://doi.org/10.1088/1748-9326/abfa4d

ENVIRONMENTAL RESEARCH
LETTERS

OPEN ACCESS

RECEIVED
18 September 2020

REVISED
24 March 2021

ACCEPTED FOR PUBLICATION
21 April 2021

PUBLISHED
11 May 2021

LETTER

Skillful prediction of tropical Pacific fisheries provided by Atlantic Niños

Iñigo Gómara[1,2,*], Belén Rodríguez-Fonseca[1,2], Elsa Mohino[1], Teresa Losada[1], Irene Polo[1] and Marta Coll[3,4]

[1] Departamento de Física de la Tierra y Astrofísica, Universidad Complutense de Madrid, 28040 Madrid, Spain
[2] Instituto de Geociencias (IGEO), UCM-CSIC, 28040 Madrid, Spain
[3] Institut de Ciències del Mar (ICM-CSIC), 08003 Barcelona, Spain
[4] Ecopath International Initiative (EII) Research Association, 08003 Barcelona, Spain
[*] Author to whom any correspondence should be addressed.

E-mail: i.gomara@ucm.es

Keywords: pantropical interactions, ENSO, Atlantic Niños, marine ecosystems, FishMIP, fisheries prediction

Supplementary material for this article is available online

Abstract

Tropical Pacific upwelling-dependent ecosystems are the most productive and variable worldwide, mainly due to the influence of El Niño Southern Oscillation (ENSO). ENSO can be forecasted seasons ahead thanks to assorted climate precursors (local-Pacific processes, pantropical interactions). However, due to observational data scarcity, little is known about the importance of these precursors for marine ecosystem prediction. Previous studies based on Earth System Model simulations forced by observed climate have shown that multiyear predictability of tropical Pacific marine primary productivity is possible. With recently released global marine ecosystem simulations forced by historical climate, full examination of tropical Pacific ecosystem predictability is now feasible. By complementing historical fishing records with marine ecosystem model data, we show herein that equatorial Atlantic sea surface temperatures (SSTs) constitute a valuable predictability source for tropical Pacific fisheries, which can be forecasted over large-scale areas up to three years in advance. A detailed physical-biological mechanism is proposed whereby equatorial Atlantic SSTs influence upwelling of nutrient-rich waters in the tropical Pacific, leading to a bottom-up propagation of the climate-related signal across the marine food web. Our results represent historical and near-future climate conditions and provide a useful springboard for implementing a marine ecosystem prediction system in the tropical Pacific.

1. Introduction

Before COVID-19, global fisheries supplied society with ∼96 million tons of fish. With 39 million people engaged in the primary sector and 4.6 million fishing vessels in operation, the fisheries industry exported USD 164 billion annually [1].

Despite the enormous anthropogenic pressure these numbers reveal, year-to-year variations in marine resources from certain oceanic regions are still largely determined by Earth's natural variability [2, 3]. This is the case of the tropical Pacific, one of the most biodiverse and productive marine areas worldwide, where El Niño Southern Oscillation (ENSO) exerts a paramount influence [4–6]. During El Niño events, weakened trade winds allow the penetration of warm waters over the central and eastern tropical Pacific, leading to suppressed equatorial and coastal upwelling of nutrient-rich waters. During La Niña these conditions reverse, inducing colder sea surface temperatures (SSTs), enhanced near-surface nutrient supply and a subsequent response of marine life [7–11].

ENSO is currently the most predictable oceanic-atmospheric variability pattern at seasonal timescales (6–12 months ahead [12]). Relevant ENSO precursors encompass local-Pacific processes [13, 14] and pantropical climate interactions [15]. Recent evidence suggests the latter are more important than previously thought in shaping ENSO evolution, intensity and structure [16–21]. Pantropical interactions are generated by recurrent SST anomaly patterns from

the tropical Atlantic and Indian oceans (e.g. equatorial and North Tropical Atlantic (NTA) [22–24], Indian Ocean Dipole [25] and Indian Ocean Basin Mode [26]). SST fluctuations have the potential to alter the Walker circulation and the surface wind regimes in the tropical Pacific [16–19, 27, 28]. However, ENSO dynamics associated with remote SST forcing are disparate.

Boreal spring NTA and autumn Indian ocean SST forcings affect the tropical Pacific mainly through oceanic temperature advection [19, 29, 30]. Although for both drivers eastward-propagating oceanic Kelvin waves are excited, in the first case SST and thermocline depth anomalies are triggered over the central Pacific [19], and in the second the main effect of Kelvin waves is through constructive interference leading to temperature advection processes [30]. Distinctively, equatorial Atlantic boreal summer anomalous SSTs (a.k.a., Atlantic Niños/Niñas) produce changes in the Pacific equatorial winds that excite eastward-propagating upwelling oceanic Kelvin waves. These waves effectively reinforce anomalies in the eastern Pacific, thereby altering the thermocline and the upwelling of ocean deep waters [31, 32]. The settled environmental conditions are, in all cases, conducive to ENSO events in the ensuing seasons, but their impact on equatorial and coastal upwelling over the eastern Tropical Pacific, where highly-productive upwelling-dependent marine ecosystems are located [1], is different [15, 23]. Thus, it is important to assess their relevance for marine ecosystem prediction, a fracture that has remained uncertain for several reasons.

Scarce, short or too local historical biological records often hinder the identification of robust statistical links between climate predictors and yield responses [33], especially when considering vast areas. Dynamical prediction by means of effectively coupled climate, biogeochemical and ecosystem models has been proven successful over multiple coastal and open sea regions [8, 34–37]. In the tropical Pacific, Earth System Model (ESM) simulations forced by observed climate have shown that multiyear predictability of tropical Pacific marine primary productivity is attainable [8, 36, 38]. These forced simulations have the benefit of reducing large SST biases present in free (unforced) runs [15, 39–41], thus allowing identification of local and remote predictability sources for eastern tropical Pacific marine ecosystems (e.g. Atlantic Niños).

With recently released global marine ecosystem models forced by observed historical climate from the Fisheries and Marine Ecosystem Model Intercomparison Project (FishMIP [42]), rigorous model-based statistical prediction can be implemented by considering the entire marine food web and its associated fisheries. Released fished and non-fished FishMIP historical simulations not only permit the effective isolation of climate-driven ecosystem responses, but also characterize the top-down control of this anthropogenic forcing.

Given the above, we evaluate herein the potential for prediction of tropical Pacific marine ecosystems and fisheries by assessing the precursory role of global SSTs. To this end, we utilize atmospheric reanalysis data, historical catch records and FishMIP simulations encompassing global marine ecosystems.

2. Materials and methods

2.1. Observational and historical ESM simulation datasets

Annual catch data from the Food and Agriculture Organization of the United Nations (FAO) major fishing areas *Eastern Central Pacific* (#77) and *Southeastern Pacific* (#87) for the period 1950–2014 were retrieved from the Sea Around Us Project (SAUP) database (www.seaaroundus.org/data/#/fao). These are a combination of official reported data from FAO FishStat database (www.fao.org/fishery/statistics/en) and reconstructed estimates of unreported data [43]. All types of marine species and fishing methods were considered altogether in the SAUP timeseries, including catches from exclusive economic zones. To retain interannual variability and minimize the potential impact of external factors (e.g. fishing effort, climate change impact) on historical catch data, a high-pass Butterworth filter with 11 year cut-off period was applied to the time series.

Observational 1° longitude-latitude SST data were retrieved from the Hadley Centre Sea Ice and Sea Surface Temperature data set (HadISST [44]). Simulated physical and biogeochemical data for the historical period (1971–2004) were obtained from the Geophysical Fluid Dynamics Laboratory (GFDL) Carbon Ocean Biogeochemistry and Lower Trophics run (COBALT [45]). Physical-biological parameters from this simulation (so-called GFDL ocean reanalysis within the FishMIP community) and additional datasets are fully described in table 1. The COBALT ocean-ice simulation, performed with the Modular Ocean Model v4p1 [46], has a 1° horizontal resolution (1/3° along the equator) and 50 vertical layers with 10 m increase in the top 200 m. The simulation is forced by air-sea fluxes from the CORE-II data set [47], a blend of the National Centers for Environmental Prediction (NCEP) atmospheric reanalysis [48] and satellite data. Whereas sea surface salinity is restored to observations in GFDL-COBALT due to drift issues, SST and biogeochemical outputs are free running (hindcasts [45, 49, 50]). Full information of the GFDL-COBALT validation against physical-biological observations (e.g. mixed layer depth, nutrient concentration, phytoplankton/zooplankton biomass, carbon/energy fluxes) is available in Stock *et al* [45].

In line with CORE-II forcing on GFDL-COBALT, NCEP reanalysis was selected to analyze atmospheric

Table 1. Description of datasets and variables considered in this study.

Dataset	Variable (acronym)	Units	Notes
Observations			
SAUP	Annual Catch	10^3 t yr^{-1}	FAO major fishing areas 77 and 87
HadISST	Sea surface temperature (SST)	K	
NCEP	Zonal, meridional and vertical winds (*u,v,w*)	m s^{-1}	From 1000 to 100 hPa
	Velocity potential (chi)	10^6 m^2 s^{-1}	0.2 sigma level
	Vertical velocity in pressure coordinates (omega)	Pa s^{-1}	From 1000 to 100 hPa
ESM historical simulation			
GFDL-COBALT	Sea surface temperature (SST)	K	
	Surface zonal and meridional currents (*uo,vo*)	m s^{-1}	
	Small and large phytoplankton production (sphy and lphy)	mol C m^{-3} s^{-1}	Vertical integral from bottom to surface
Marine ecosystem model historical simulations (column-integrated outputs; ISIMIP2a simulation protocol)			
EcoOcean	Total system carbon biomass density (tsb)	g C m^{-2}	All primary producers and consumers
	Total consumer carbon biomass density (tcb)	g C m^{-2}	Trophic level >1, invertebrates and vertebrates
	Carbon biomass density of consumers greater than 10 cm (b10) and 30 cm (b30)	g C m^{-2}	b10 include b30
	Carbon biomass density of commercial species (bcom)	g C m^{-2}	Harvested fish greater than 10 cm; fishing scenario
	Total catch at sea (tc)	g wet biomass m^{-2}	Commercial landings, discards, fish and invertebrates; fishing scenario
BOATS	Total consumer carbon biomass density (tcb)	g C m^{-2}	Only commercial species
	Biomass density of small (bsmall), medium (bmed) and large size (blarge) consumers	g C m^{-2}	
	Total catch at sea (tc)	g wet biomass m^{-2}	Fishes excluding invertebrates; fishing scenario
Macroecological	Total consumer carbon biomass density (tcb)	g C m^{-2}	Annual average. Only commercial species
	Carbon biomass density of consumers greater than 10 cm (b10) and 30 cm (b30)	g C m^{-2}	Annual average, b10 include b30

circulation dynamics and variability in this work (cf table 1).

2.2. Fisheries and marine ecosystem model simulations

Model simulations from the FishMIP v1 intercomparison protocol [42] were analyzed. Available model outputs through the ISIMIP repository (https://esg.pik-potsdam.de/search/isimip/) were considered for the analysis: EcoOcean, BOATS and Macroecological [51].

EcoOcean is a complex spatial-temporal global ecosystem model that comprehensively simulates interactions within all trophic levels and species groups using the Ecospace [52] spatial-temporal model at its core. The depth dimension is implicitly considered in the model by preferent habitat patterns and food-web interactions (one dimensional). EcoOcean v1 uses SAUP effort data [53] spatially distributed across large marine ecosystem regions as fishing forcing. Effort data combine fleet information (e.g. number and type of boats) and dedicated time for fishing. The forcing is applied as a mortality rate for functional groups in the simulation through the removal of existing biomass per unit of time. The model is able to replicate historical catch successfully on a global scale. A full description of EcoOcean is available in Christensen *et al* [54].

BOATS is a global ecological model that determines size spectra of fish biomass as a function of net primary production and local temperature. Biomass production in higher trophic levels is limited by available photosynthetic energy, temperature-dependent

Table 2. Description of available FishMIP simulations analyzed and scenario acronyms.

Model	Resolution	Diazotrophs	Forcing	Period	Fishing	Acronym
EcoOcean	1° × 1° Monthly	Yes	GFDL-COBALT	1971–2004	SAUP effort	EcoG-Fis
					No	EcoG
			IPSL-CM5A-LR RCP 8.5	2021–2054	SAUP effort 2005	EcoI8.5-Fis
		No	GFDL-COBALT	1971–2004	SAUP effort	EcoG-Fis-wodiaz
BOATS	1° × 1° Monthly	No	GFDL-COBALT	1971–2004	SAUP catch price	BoaG-Fis
					No	BoaG
Macroecological	1° × 1° Yearly	Yes	GFDL-COBALT	1971–2004	No	MacG

growth rates and trophic efficiency scaling. The model enables a realistic representation of biological and ecological processes, allowing evaluation of the links between climate, biogeochemistry and upper trophic dynamics. BOATS employs a bioeconomic approach based on SAUP catch price data to determine spatial-temporal changes in fishing efforts. The vertical dimension is a single surface-integrated layer and movement of fish is disregarded. Full information on the model architecture is available in Carozza *et al* [55].

Macroecological is a static-equilibrium model that relies on predator-prey mass ratios, transfer efficiency and metabolic demands dependent on body mass and temperature to predict size and distribution of marine consumers (as a whole) at any given time and location. It has a single vertical (surface-integrated) layer and movement of fish is disregarded. Extended information on the model is available in Jennings and Collingridge [56].

Seven different simulations were analyzed in this study. These include fished and unfished runs with and without diazotrophs dynamics (table 2). All historical runs (1971–2004) are forced by GFDL-COBALT simulation, whereas an EcoOcean 2021–2054 projection is driven by IPSL-CM5A-LR RCP8.5 [57]. In the latter, fishing forcing is kept constant at 2005 rates [42]. Although GFDL-ESM2M was also available as driving forcing for 2021–2054, it was eventually disregarded due to its inability to simulate a connection reminiscent of the observed Atlantic-Pacific teleconnection subject of this study [58]. Complete information on simulation settings, acronyms and data sources are available in table 2. All common FishMIP model output variables considered are detailed in table 1 and are publicly available through the FishMIP global model repository [51]. The most detailed model simulation (EcoOcean) forced by historical fisheries effort and which includes diazotrophs dynamics is used as reference throughout the manuscript (hereafter EcoG-Fis), as it provides the closest possible approximation to reality.

2.3. Physical-biological indices and statistical methods

Monthly anomalies of physical-biological variables were calculated by removing their total period average to the time series of each grid point. Seasonal (4 month) anomalies were computed as aggregated monthly anomalies, with linear trends effectively removed to minimize the impact of anthropogenic climate change [59].

Physical-biological indices were determined by spatially averaging seasonal anomalies over regions of interest, e.g. Niño3 (150° W–90° W, 5° S–5° N) and Atl3 (20° W–0° E, 3° S–3° N). All indices were normalized by dividing the time series by their standard deviation.

Whereas Atl3 was computed for SST on boreal summer (July–September; JJAS) to represent Atlantic Niño variability during its peak intensity [22] (a.k.a. Atlantic Equatorial Mode), Niño3 and global seasonal anomalies of physical-biological variables (cf table 1) were calculated as rolling 4 month averages between monthly lags −8 to 24, where lag 0 corresponds to JJAS, lag 1 (−1) to JASO (MJJA) of the same calendar year and so forth (back).

Statistical significance for correlation outputs (figures 1, 3 and 4; 95% confidence interval) was evaluated using a Student-t test that accounts for the autocorrelation of the time series and the calculation of effective degrees of freedom [60].

2.4. S4CAST model

The SST-based Statistical Seasonal forecast model (S4CAST) is a novel statistical seasonal model that utilizes SST data (predictor) to forecast the response of any given impact variable (predictand). To this end, the model performs a maximum covariance analysis (MCA [61]) between a predictor Y field (SST anomalies) and a predictand Z field for any given region, time period and lag.

MCA is based on single value decomposition applied to the non-square covariance matrix (C) of both Y and Z fields. The method calculates linear

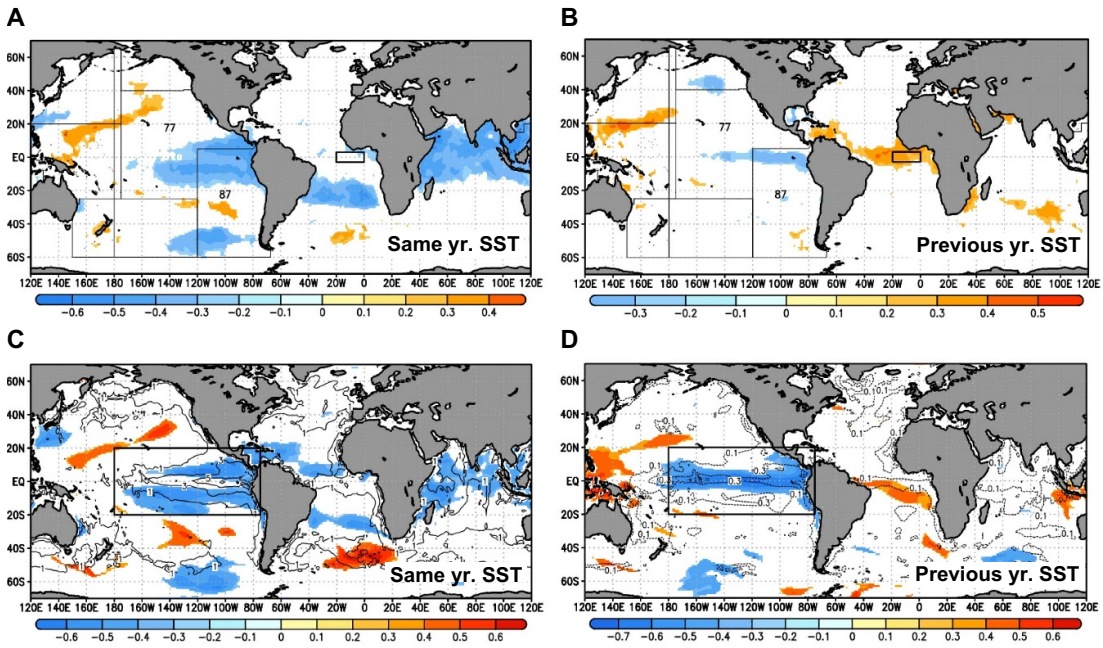

Figure 1. Links between Pacific total catch and global SSTs. (A) Correlation between interannual Sea Around Us Project historical catch (FAO aggregated 77 and 87 areas) anomalies and concomitant SST (HadISST) anomalies (shadings; p-value < 0.05). Period 1950–2014. Box for Atl3 SST index calculation in black rectangle. (B) Same as (A) but for correlation with previous calendar year SST anomalies. (C) Correlation between interannual tropical Pacific averaged (black rectangle) simulated historical total catch anomalies from EcoOcean model (EcoG-Fis simulation) and concomitant SST anomalies from GFDL-COBALT (shadings; p-value < 0.05). Period 1971–2004. Annual averaged carbon biomass density of commercial species (*bcom*) from EcoOcean model in contours. (D) Same as (C) but for correlation with previous calendar year SST anomalies (shadings) and standard deviation of annual bcom (contours).

combinations of the time series of Y and Z (a.k.a. expansion coefficients U and V, respectively) to maximize C.

A leave-one-out cross-validated hindcast based on MCA outputs is then performed [62]. For this purpose, predictor/predictand data combinations from all years except the year being predicted at each training stage are selected for model training and validation [62, 63]. A Monte Carlo test with 1000 random permutations is applied to MCA (U vs. anomalous field correlations) and cross-validation of skill scores for hypothesis testing (95% confidence interval). The Pearson correlation coefficient is selected as a qualitative indicator for model skill (sign of response).

Further details on the S4CAST statistical model framework are available in Suárez-Moreno and Rodríguez-Fonseca [64].

3. Results

3.1. Global SST relationship with tropical Pacific fisheries

We find year-to-year variations of historical global SSTs and eastern Pacific total catch records from the SAUP database (FAO areas 77 and 87) robustly correlated for the period 1950–2014. The years when observed fish catches are higher than usual synchronize with well-developed La Niña-like SST anomalies over the tropical Pacific and elsewhere [11, 65] (figure 1(A)). Lagged SST anomalies from the previous calendar year depict a preceding Atlantic Niño signal, together with a developing La Niña over the Pacific (figure 1(B)).

Likewise, we consider EcoOcean model historical simulation in a fishing forcing scenario (EcoG-Fis) for the same analysis. We first characterize the tropical Pacific in terms of biomass density of commercial species. As expected, this is the most productive and fluctuating region worldwide in the model (figures 1(C) and (D)). Despite the slightly smaller area and shorter period considered (FishMIP coverage; 1971–2004), results very similar to observations are obtained from the model (figures 1(C) and (D)). Apart from equatorial Atlantic SST anomalies and intrinsic 2–7 years Niña-Niño intermittency, no other significant relations with tropical SST anomalies (e.g. NTA, Indian) are found, either in observations or in simulations during the years preceding annual-averaged total catch anomalies (figure 1 and supplementary material figure S1 (available online at stacks.iop.org/ERL/16/054066/mmedia)).

Correlation between the Atlantic Niño index (Atl3 JJAS SST; hereafter Atl3-Had) and the tropical Pacific total catch corroborates the lagged one year Atlantic-Pacific relationship in the model and observations (supplementary material figure S2). As expected, this relationship substantially weakens and

changes sign in subsequent year lags. In agreement with Rodríguez-Fonseca *et al* [16], a slightly stronger Atlantic-Pacific connection is found for 1971–2004 compared to 1950–2014.

3.2. Statistical prediction of tropical Pacific total catch using equatorial Atlantic SSTs

Owing to constraints in historical fishing records (averaged annual data over vast areas), we focus on gridded 1-degree monthly FishMIP modeling outputs for fisheries prediction. Again, we consider the most detailed model forced by historical fisheries efforts (EcoG-Fis), which provides the closest approximation to reality (table 2). We then use the Sea Surface temperature-based Statistical Seasonal forecast model (S4CAST [64]) to perform a cross-validated hindcast of simulated tropical Pacific marine yields: total catch at sea (tc) and total system carbon biomass density (tsb).

Consistent with figure 1, we use as predictor (Y) equatorial Atlantic SST anomalies during the peak intensity season (Atl3 JJAS-lag 0) of Atlantic Niños/Niñas [16, 22, 66] on GFDL-COBALT, the driving historical forcing of FishMIP. Tropical Pacific (150° W–75° W, 20° S–20° N) simulated total catch and total system biomass anomalies are used as predictands (Z) for different monthly lagged periods (0 to 42).

For all monthly lags, Atlantic Niño emerges as the main predictor of tropical Pacific total catch anomalies, which can be hindcasted over large-scale areas and up to three years in advance (figures 2(A)–(E) and supplementary material figure S3). The quantification of the surface area of the domain with skillful prediction returns values of up to 3.4 million km^2 at lag 20 (figure 2(F)). If total system carbon biomass density is considered as predictand (Z) instead of total catch, final results are very similar but shifted ∼9–12 months back in time (compare supplementary material figures S3 and S4), with a maximum of 4.2 million km^2 of surface area with skillful prediction at lag 8 (figure 2(F)).

3.3. Atlantic-Pacific physical-biological mechanism

To establish a physical-biological mechanism explaining the results above, we evaluate tropical Atlantic (Atl3) SST impact on Pacific (Niño3) region for different area-averaged physical-biological variables and monthly lags. The simulation selected for this purpose is again EcoG-Fis, although other marine ecosystem models (BOATS, Macroecological) and scenarios are also considered (cf tables 1, 2 and Tittensor *et al* [42]).

First, we check whether the Atlantic-Pacific physical teleconnection is realistically represented in GFDL-COBALT. This is motivated by the fact that SSTs are not restored to observations in the simulation and equatorial wind fields in CORE-II depict inaccuracies [50, 67]. Particularly, inconsistencies in wind speed, humidity, and solar radiation have been reported between NCEP and CORE-II [47]. In spite of this, the good performance of GFDL-COBALT representing Atlantic Niño variability and associated impacts is confirmed in figure 3(A) and supplementary material figure S5, where results obtained are very similar to observational studies [16, 28]. For a warming in the equatorial Atlantic, a strengthening of the Pacific Walker Circulation is observed, together with increased subsidence and anomalous easterlies over the western equatorial Pacific, features that promote subsequent La Niña conditions (supplementary material figure S5). Similarly, previous studies have shown that anomalous easterly winds over the western equatorial Pacific promote the propagation of equatorial upwelling Kelvin waves [23, 31, 32, 68], thus favoring the emergence of nutrients from the seabed.

The linear correlation value between Atlantic Niño indices (Atl3 JJAS 1971–2004) in GFDL-COBALT and HadISST is 0.87, whereas that for Niño3 (NDJF) is 0.96 (p-values < 0.05). The fact that both SST variabilities are significantly governed by the movement of water in response to wind variations may be behind the good agreement between GFDL-COBALT and HadISST [39, 49].

Lagged-correlations for biological variables in figure 3(A) enable characterization of the bottom-up propagation of Atl3-related signal (hereafter Atl3-GF) across the Niño3 region food web. Closely synchronous to the growth of cold nutrient-rich SST anomalies (figure 3(A)), large phytoplankton production (lphy), total system (tsb) and total consumer (tcb) carbon biomass densities grow rapidly before monthly lag 0, and decay thereafter at different rates. The different declining rates are due to distinct variable definitions and growth rates of species included in each category. While lphy is large-phytoplankton dependent, tcb is dominated by zooplankton and *tsb* is a blend of both (cf table 1). Consistent with previous studies [69], we find no SST response by small phytoplankton (not shown). Variables negative lag behavior can be partially explained by construction of Atl3 index at its peak season instead of its growing stage (supplementary material figure S6), and the fact that ocean chlorophyll tends to slightly precede ENSO-related SST anomalies due to wind-iron supply dynamics [70].

Results for carbon biomass density of fish consumers greater than 10 cm (b10) and 30 cm (b30) depict a bottom-up propagation of the physical forcing over time, peaking ∼9–12 months later than large phytoplankton productivity (figure 3(A)). By construction of b10/b30, where fish species are classified in terms of body size, bottom-up indirect effects of climate anomalies seem to overbalance species-specific direct temperature-recruitment processes [65]. A feasible process for this bottom-up propagation is a recruitment increase of short-lived

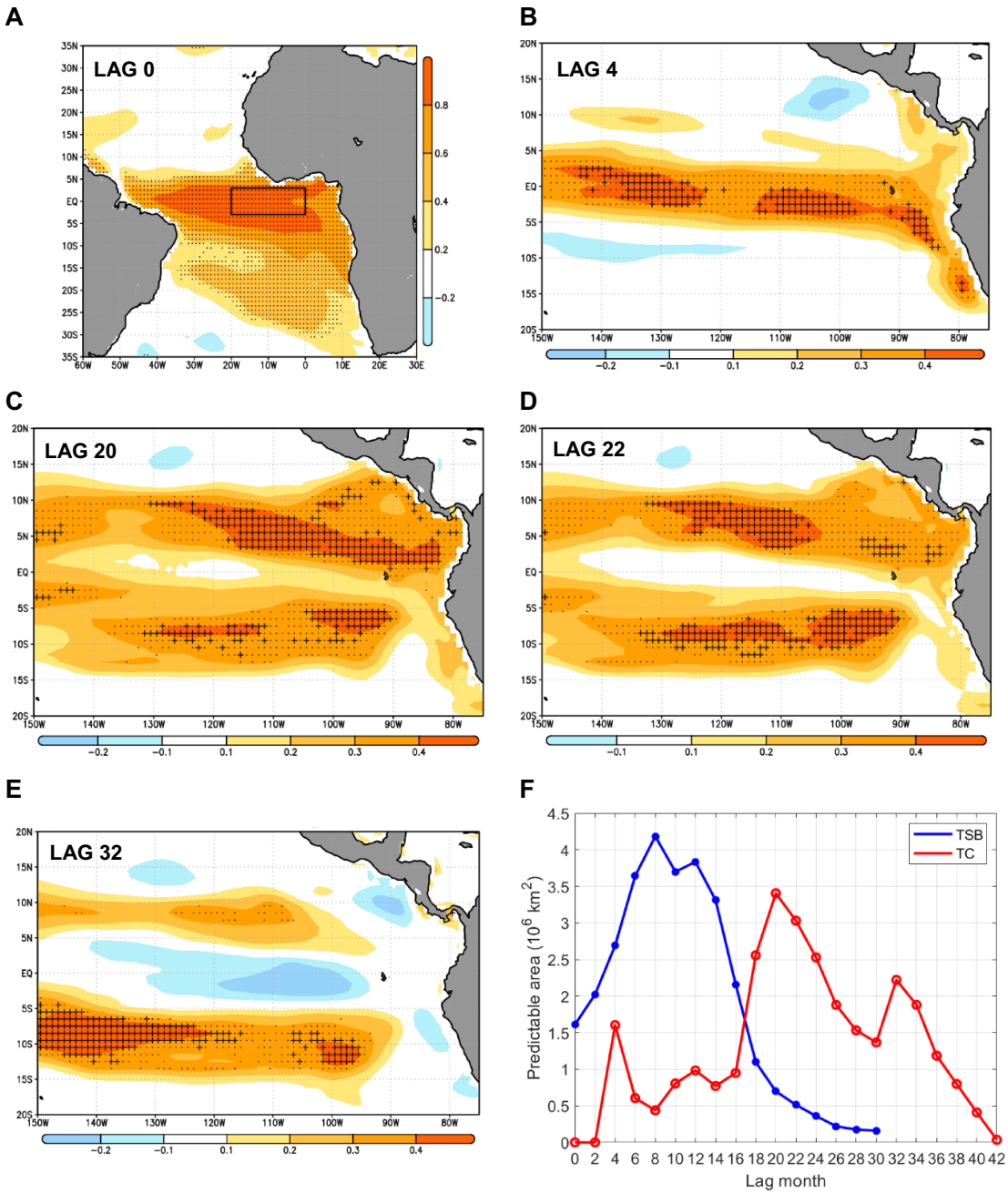

Figure 2. Hindcasts of tropical Pacific total catch based on Atlantic SSTs. Co-variability maps corresponding to the leading maximum covariance analysis (MCA) modes between equatorial Atlantic lag 0 SST anomalies (predictor; Atl3 region (20° W–0° E, 3° S–3° N)—black box) and tropical Pacific total catch (tc) at sea at different monthly lags (predictand; (150° W–75° W, 20° S–20° N)). (A) Homogeneous map obtained by regression of SST anomalies on monthly lag 0 (JJAS) on expansion coefficient U (equivalent to Atlantic Niño index). *P*-values <0.05 in SST-U correlation in stippling (Monte Carlo test with 1000 random permutations). (B) Heterogeneous map obtained by regression of tropical Pacific *tc* anomalies on monthly lag 4 (ONDJ) on U. P-values <0.05 in *tc*-U correlation in stippling. Cross-validated anomaly correlation skill scores calculated from the MCA between hindcasts and simulated *tc* in crosses (95% confidence interval). (C)–(E) Same as (B) but for monthly lags 20 (FMAM), 22 (AMJJ) and 32 (FMAM). (F) Evolution of surface area with skillful prediction (crosses in (B)–(E)) for total catch (tc) and total system biomass (tsb) from lags 0 to 42 (10^6 km^2). Period 1971–2004. EcoG-Fis simulation. See section 2 for further information on MCA.

species caused by enhanced food supply at lower trophic levels [36].

The spatial response of physical-biological variables for lags 0, 9 and 24 is shown in figures 3(B)–(D). At lag 0, cold SST anomalies and enhanced lphy/tsb are present over the Niño3 region (figure 3(B)). At lag 9, a mature La Niña is present, together with increased b10 over the Niño3 area and lphy/tsb to the north and south. This northward-southward advection of lphy appears related to Ekman transport induced by enhanced trade winds (supplementary material figure S7). At lag 24 increased b10 also appears displaced to the north and south, while b30 is only located to the north.

A broader picture of this evolution is given in figure 4 in the form of Hovmöller diagrams.

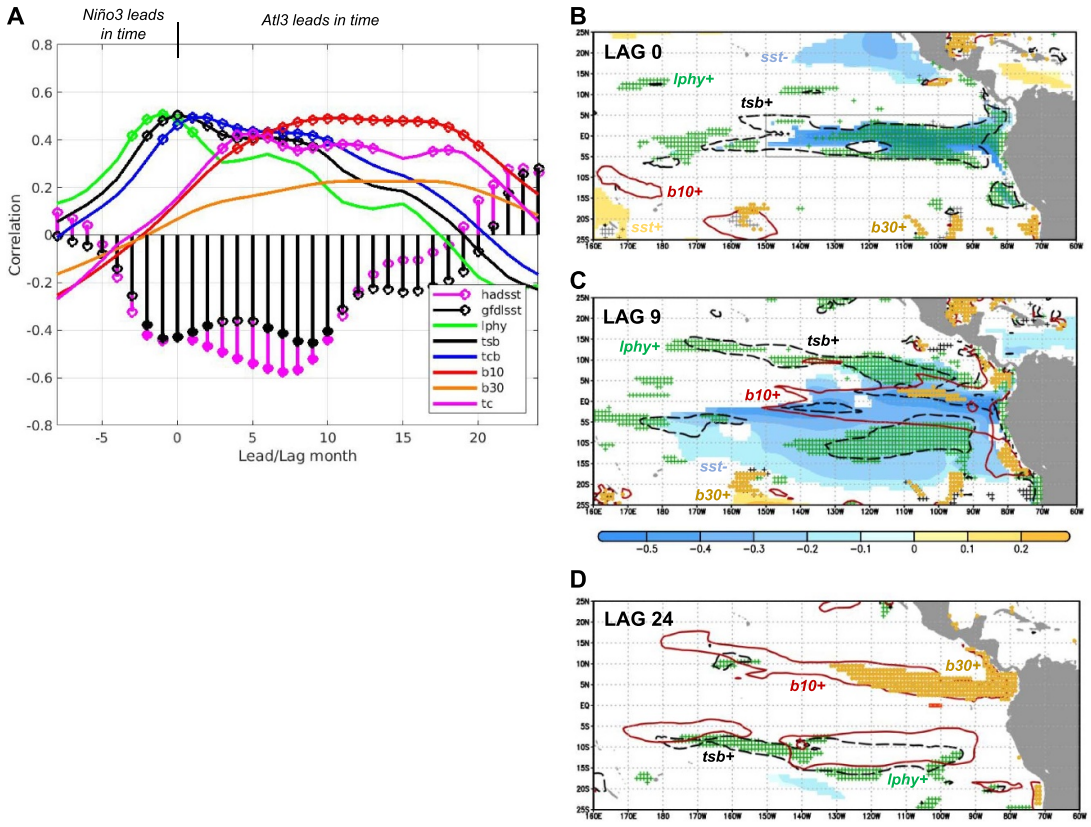

Figure 3. Atlantic-Pacific physical-biological mechanism. (A) Correlation between Atl3-GF index and lagged (−6 to 24) Niño3 rolling 4 month anomalies of SST, large phytoplankton production (lphy), total system carbon biomass density (tsb), total consumer carbon biomass density (tcb), carbon biomass density of consumers greater than 10 cm (b10) and 30 cm (b30) and total catch at sea (tc). *P*-values <0.05 in markers (see legend). (B) Regression of tropical Pacific lag 0 SST anomalies (shadings; in K) on Atl3-GF index, and correlation of lphy (green crosses), tsb (black dashed contours), b10 (red contours) and b30 (orange xs) anomalies with the same index. Only *p*-values <0.05 for positive correlations are shown, except for SST (see text labels). Niño3 region highlighted in thin rectangle. (C) Same as (B) but for monthly lag 9. (D) Same as (B) but for monthly lag 24. Period 1971–2004. GFDL-COBALT and EcoG-Fis simulations.

Enhanced lphy/tsb/tcb tend to overlap with cold SST anomalies, preserving the timing from figure 3(A). Growth starts at small negative lags over the central tropical Pacific, then anomalies propagate to the east until lag 3 (figure 4(A)) and split thereafter into two branches to the north and south (figure 4(B)). The long persistence of lphy/tsb/tcb anomalies may be caused by enduring presence of nutrients (nitrate and dissolved iron). As opposed to SSTs, surface nutrients do not interact with the atmosphere [8, 36]. Lastly, whereas b10 show a similar response to lphy ∼9 months later, increased b30 are constrained over the northeast tropical Pacific from lags 14 to 24 (figures 3(D) and 4(B)). The latter may be caused by regional currents disposition leading to latitudinal asymmetries in large fish abundance (cf contours in figure 1(C) as a hint). Nevertheless, a species-specific analysis (beyond the scope of this letter) is needed to answer this question.

The evolution of physical-biological variables shown in figures 3 and 4 are in line with the shape and progression of total catch and total system biomass predictable regions in figure 2 (large crosses) and supplementary material figures S3 and S4. This is consistent with the propagation in time of climate anomalies within the food web.

To evaluate the role of diazotrophs dynamics in the physical-biological mechanism, the analysis in figure 4 is replicated in the EcoG-fis-wodiaz simulation (identical to EcoG-fis but without diazotrophs dynamics, cf table 2). The differences obtained between the two simulations are exiguous and therefore not shown. This seems consistent with the fact that primary production linked to nitrogen fixation is much less compared to total primary production, particularly in highly-productive marine areas [42, 71, 72].

To test the sensitivity of ecosystem response to top-down fishing control and model setup, in supplementary material figures S8–S10 we perform the same analyses on EcoOcean and BOATS fished and unfished model output scenarios (table 2). Results indicate that climate-driven bottom-up propagation dominates the response throughout the trophic web,

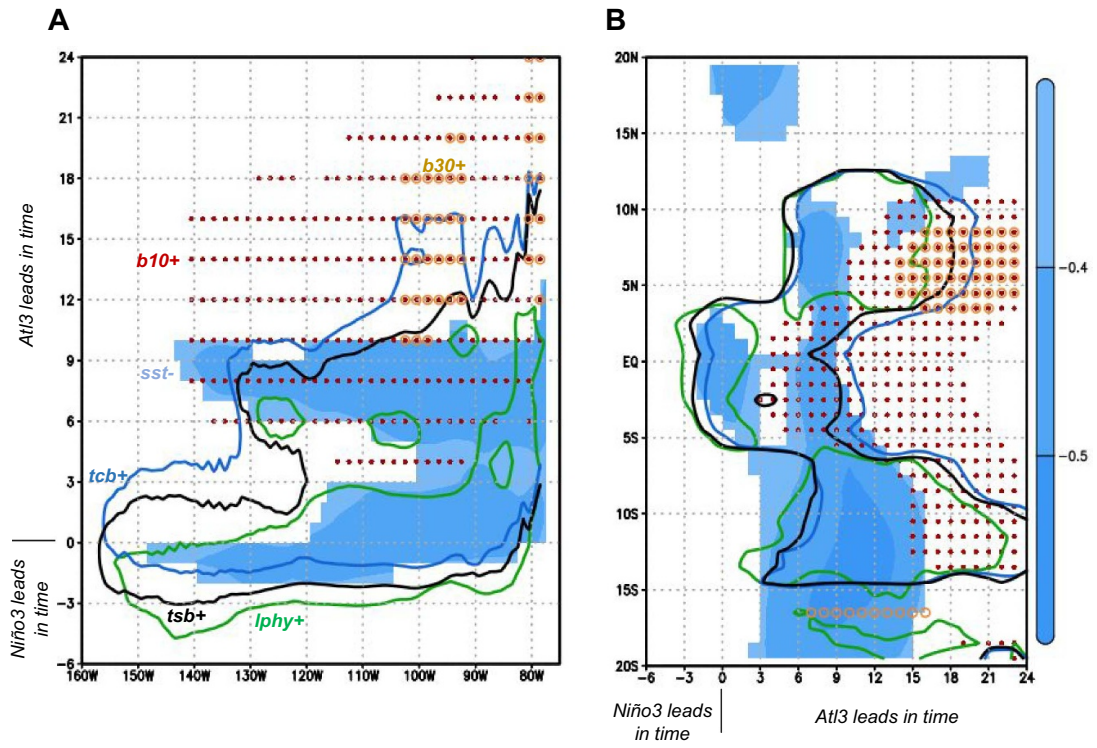

Figure 4. Atlantic-Pacific physical-biological mechanism. Hovmöller diagrams. (A) Regression of meridionally averaged (5° S–5° N) rolling four month anomalies of SST (shadings; in K) on Atl3-GF index, and correlation of meridionally averaged large phytoplankton production (lphy; green contours), total system carbon biomass density (tsb; black contours), total consumer carbon biomass density (tcb; blue contours) and carbon biomass density of consumers greater than 10 cm (b10; red dots) and 30 cm (b30; orange circles) with the same index. Only p-values <0.05 for positive correlations are shown, except for SST (see text labels). Lags −6 to 24. (B) Same as (A) but for zonally averaged anomalies (150° W–75° W). Period 1971–2004. GFDL-COBALT and EcoG-Fis simulations.

while fishing visibly affects large predators over large-scale areas. The differences observed between models (less persistent and westward displaced anomalies of all-size fish biomasses in BOATS model outputs) may be caused by different model complexity, internal hypothesis regarding species dynamics and species relationships, ecosystem functioning and fisheries schemes [42, 59].

Lastly, a similar analysis is conducted for Macroecological, although it only provides annual model outputs, does not include a fishing scenario, and propagation in time of anomalies through the food chain is unresolved (supplementary material figure S11). As expected, the model returns the same picture as in figures 3(B) and (C) for lagged years 0 and 1, with the difference that consumer response (tcb/b10/b30) to the forcing is no longer lagged in time.

4. Summary and discussion

In this work, the predictability of seasonal to multiannual tropical Pacific marine ecosystem resources was investigated on observations (SAUP catch data) and ecosystem model simulations (FishMIP). Evidence indicates that tropical Pacific fisheries can be forecasted over large-scale areas, and up to three years in advance, by solely considering boreal summer equatorial Atlantic SST anomalies (Atlantic Niños/Niñas) as predictor.

The outstanding skill for predicting Pacific fisheries provided by Atlantic Niños/Niñas can be attributed to the dynamical processes they trigger in the tropical Pacific. These processes involve the alteration of upwelling conditions by anomalous surface winds through the propagation of equatorial Kelvin waves [31, 32]. Contrastingly, other well-known remote SST ENSO precursors are associated with more advective processes over the western and central Pacific [19, 30] (e.g. NTA, Indian Ocean Dipole), which do not seem to have a substantial impact on highly-productive upwelling-dependent marine ecosystems located further to the east in the basin. These results highlight the importance of equatorial Atlantic impact on ENSO [16, 28, 68, 73].

This study is also supported by previous works that laid foundations for skillful seasonal to multiyear predictability of marine primary productivity in the tropical Pacific [8, 36, 38]. By providing an extension for these analyses across the entire marine food web and identifying its predictability sources, the results presented here may contribute to a more sustainable management of fisheries in the region.

It remains uncertain whether the described biophysical Atlantic-Pacific relation will persist in the future. It is envisaged that under greenhouse warming conditions biomass over the tropical oceans will decline [59], strong eastern ENSO events will become more likely [74] and the Atlantic-Pacific teleconnection (nonstationary in nature [16, 32]) will weaken [58]. Furthermore, future scenarios for fisheries are currently even more uncertain than pre-COVID-19 ones [75].

Although disentangling the interplay of all these factors may require a suite of sensitivity experiments beyond the scope of this study, we provide exploratory results for the period 2021–2054 in supplementary material figure S12 (RCP8.5 fished scenario; cf table 2). Overall, results analogous to those obtained for the historical period are found, supporting the applicability of our findings for the decades to come.

Nevertheless, we simply propound a few possible alternative approaches to marine ecosystem modeling. When additional FishMIP simulations become available, a more comprehensible picture may unfold.

Data availability statement

Annual catch data from FAO major fishing areas are available from the Sea Around Us Project (www.seaaroundus.org/data/#/fao). Hadley Centre Sea Ice and Sea Surface Temperature data set (HadISST) are available from the Met Office Hadley Centre observations datasets (www.metoffice.gov.uk/hadobs/hadisst/). National Centers for Environmental Prediction (NCEP) reanalysis data are available from the NOAA/OAR/ESRL PSL website (https://psl.noaa.gov/). GFDL-COBALT and FishMIP simulation data (EcoOcean, BOATS and Macroecological) are accessible through the Potsdam-Institute for Climate Impact Research Earth System Grid Federation (ESGF) data node (https://esg.pik-potsdam.de/search/isimip/).

Acknowledgments

This research was funded by the EU H2020 project TRIATLAS (No. 817578), the Universidad Complutense de Madrid project FEI-EU-19-09 and the Spanish Ministry of Economy and Competitiveness project PRE4CAST (CGL2017-86415-R). This work also acknowledges the 'Severo Ochoa Centre of Excellence' accreditation by the Spanish Ministry of Science and Innovation (CEX2019-000928-S) to the Institute of Marine Science (ICM-CSIC). We thank Derek Tittensor (UNEP-WCMC) and Iliusi Vega (PIK-Postdam) for help with FishMIP data extraction. We thank Roberto Suárez-Moreno (LDEO-Columbia University), Jeroen Steenbeek (ICM-CSIC) and Charles Stock (NOAA-GFDL) for their cooperation and help during the progress of this study. Finally, we would like to thank the two anonymous reviewers for their helpful comments and suggestions, which contributed to improve this manuscript.

Code availability

S4CAST originally published MATLAB® code is open-access and available from the Zenodo repository (doi:10.5281/zenodo.15985) in the URL https://zenodo.org/record/15985. The rest of MATLAB scripts used in this analysis can be made available upon request from the corresponding author (i.gomara@ucm.es). Updated S4CAST versions can be requested to the TROPA-UCM research group (brfonsec@ucm.es).

ORCID iDs

Iñigo Gómara https://orcid.org/0000-0001-8721-0307
Belén Rodríguez-Fonseca https://orcid.org/0000-0002-5261-7083
Elsa Mohino https://orcid.org/0000-0002-4342-6349
Teresa Losada https://orcid.org/0000-0002-8430-1745
Irene Polo https://orcid.org/0000-0002-6250-6109
Marta Coll https://orcid.org/0000-0001-6235-5868

References

[1] FAO 2020 *The State of World Fisheries and Aquaculture 2020. Sustainability in action* (Rome: Food and Agriculture Organization of the United Nations) (https://doi.org/10.4060/ca9229en)
[2] Drinkwater K F, Beaugrand G, Kaeriyama M, Kim S, Ottersen G, Perry R I, Pörtner H-O, Polovina J J and Takasuka A 2010 On the processes linking climate to ecosystem changes *J. Mar. Syst.* **79** 374–88
[3] Ottersen G, Kim S, Huse G, Polovina J J and Stenseth N C 2010 Major pathways by which climate may force marine fish populations *J. Mar. Syst.* **79** 343–60
[4] Philander S G 1990 *El Niño, La Niña, and the Southern Oscillation* (New York: Academic) pp ix, 293
[5] McPhaden M J, Zebiak S E and Glantz M H 2006 ENSO as an integrating concept in earth science *Science* **314** 1740–5
[6] Bertrand A *et al* 2020 El Niño Southern Oscillation (ENSO) effects on fisheries and aquaculture *FAO Fisheries and Aquaculture Technical Paper*
[7] Boyce D G, Lewis M R and Worm B 2010 Global phytoplankton decline over the past century *Nature* **466** 591–6
[8] Seferian R, Bopp L, Gehlen M, Swingedouw D, Mignot J, Guilyardi E and Servonnat J 2014 Multiyear predictability of tropical marine productivity *Proc. Natl Acad. Sci.* **111** 11646–51
[9] Polovina J J, Howell E A, Kobayashi D R and Seki M P 2017 The Transition Zone Chlorophyll Front updated: advances from a decade of research *Prog. Oceanogr.* **150** 79–85
[10] Brainard R E *et al* 2018 Ecological impacts of the 2015/16 El Niño in the central equatorial Pacific *Bull. Am. Meteorol. Soc.* **99** S21–S6

[11] Chavez F P et al 1999 Biological and chemical response of the equatorial Pacific Ocean to the 1997–98 El Niño Science 286 2126
[12] Barnston A G, Tippett M K, L'Heureux M L, Li S and DeWitt D G 2012 Skill of real-time seasonal ENSO model predictions during 2002–11: is our capability increasing? Bull. Am. Meteorol. Soc. 93 631–51
[13] Meinen C S and McPhaden M J 2000 Observations of warm water volume changes in the equatorial Pacific and their relationship to El Niño and La Niña J. Clim. 13 3551–9
[14] Harrison D E and Chiodi A M 2015 Equatorial Pacific easterly wind surges and the onset of La Niña Events* J. Clim. 28 776–92
[15] Cai W et al 2019 Pantropical climate interactions Science 363 eaav4236
[16] Rodríguez-Fonseca B, Polo I, García-Serrano J, Losada T, Mohino E, Mechoso C R and Kucharski F 2009 Are Atlantic Niños enhancing Pacific ENSO events in recent decades? Geophys. Res. Lett. 36 L20705
[17] Losada T, Rodríguez-Fonseca B, Polo I, Janicot S, Gervois S, Chauvin F and Ruti P 2010 Tropical response to the Atlantic equatorial mode: AGCM multimodel approach Clim. Dyn. 35 45–52
[18] Ding H, Keenlyside N S and Latif M 2012 Impact of the equatorial Atlantic on the El Niño Southern Oscillation Clim. Dyn. 38 1965–72
[19] Ham Y-G, Kug J-S, Park J-Y and Jin F-F 2013 Sea surface temperature in the north tropical Atlantic as a trigger for El Niño/Southern Oscillation events Nat. Geosci. 6 112–6
[20] McGregor S, Timmermann A, Stuecker M F, England M H, Merrifield M, Jin F-F and Chikamoto Y 2014 Recent Walker circulation strengthening and Pacific cooling amplified by Atlantic warming Nat. Clim. Change 4 888–92
[21] Dommenget D and Yu Y 2016 The effects of remote SST forcings on ENSO dynamics, variability and diversity Clim. Dyn. 49 2605–24
[22] Zebiak S E 1993 Air–sea interaction in the equatorial Atlantic Region J. Clim. 6 1567–86
[23] Ham Y-G, Kug J-S and Park J-Y 2013 Two distinct roles of Atlantic SSTs in ENSO variability: north tropical Atlantic SST and Atlantic Niño Geophys. Res. Lett. 40 4012–7
[24] Enfield D B and Mayer D A 1997 Tropical Atlantic sea surface temperature variability and its relation to El Niño-Southern Oscillation J. Geophys. Res. Oceans 102 929–45
[25] Saji N H, Goswami B N, Vinayachandran P N and Yamagata T 1999 A dipole mode in the tropical Indian Ocean Nature 401 360–3
[26] Yang J, Liu Q, Xie S-P, Liu Z and Wu L 2007 Impact of the Indian Ocean SST basin mode on the Asian summer monsoon Geophys. Res. Lett. 34 L02708
[27] Latif M and Barnett T P 1995 Interactions of the tropical oceans J. Clim. 8 952–64
[28] Wang C 2006 An overlooked feature of tropical climate: inter-Pacific-Atlantic variability Geophys. Res. Lett. 33 L12702
[29] Kug J-S and Kang I-S 2006 Interactive feedback between ENSO and the Indian Ocean J. Clim. 19 1784–801
[30] Izumo T, Vialard J, Lengaigne M, De Boyer Montegut C, Behera S K, Luo J-J, Cravatte S, Masson S and Yamagata T 2010 Influence of the state of the Indian Ocean Dipole on the following year's El Niño Nat. Geosci. 3 168–72
[31] Polo I, Martin-Rey M, Rodriguez-Fonseca B, Kucharski F and Mechoso C R 2015 Processes in the Pacific La Niña onset triggered by the Atlantic Niño Clim. Dyn. 44 115–31
[32] Martín-Rey M, Rodríguez-Fonseca B and Polo I 2015 Atlantic opportunities for ENSO prediction Geophys. Res. Lett. 42 6802–10
[33] Myers R A 1998 When do environment–recruitment correlations work? Rev. Fish Biol. Fish. 8 285–305
[34] Stock C A et al 2015 Seasonal sea surface temperature anomaly prediction for coastal ecosystems Prog. Oceanogr. 137 219–36
[35] Hobday A J, Spillman C M, Paige Eveson J and Hartog J R 2016 Seasonal forecasting for decision support in marine fisheries and aquaculture Fish. Oceanogr. 25 45–56
[36] Park J-Y, Stock C A, Dunne J P, Yang X and Rosati A 2019 Seasonal to multiannual marine ecosystem prediction with a global Earth system model Science 365 284
[37] Di Lorenzo E and Ohman M D 2013 A double-integration hypothesis to explain ocean ecosystem response to climate forcing Proc. Natl Acad. Sci. 110 2496
[38] Ham Y-G, Joo Y-S and Park J-Y 2021 Mechanism of skillful seasonal surface chlorophyll prediction over the southern Pacific using a global earth system model Clim. Dyn. 56 45–64
[39] Doney S C, Yeager S, Danabasoglu G, Large W G and McWilliams J C 2007 Mechanisms governing interannual variability of upper-ocean temperature in a global ocean hindcast simulation J. Phys. Oceanogr. 37 1918–38
[40] Wang C, Zhang L, Lee S-K, Wu L and Mechoso C R 2014 A global perspective on CMIP5 climate model biases Nat. Clim. Change 4 201–5
[41] Kucharski F, Syed F S, Burhan A, Farah I and Gohar A 2014 Tropical Atlantic influence on Pacific variability and mean state in the twentieth century in observations and CMIP5 Clim. Dyn. 44 881–96
[42] Tittensor D P et al 2018 A protocol for the intercomparison of marine fishery and ecosystem models: fish-MIP v1.0 Geosci. Model Dev. 11 1421–42
[43] Pauly D, Zeller D and Palomares M L D (eds) 2020 Sea Around Us Concepts, Design and Data
[44] Rayner N A et al 2003 Global analyses of sea surface temperature, sea ice, and night marine air temperature since the late nineteenth century J. Geophys. Res. Atmos. 108 D14, 4407
[45] Stock C A, Dunne J P and John J G 2014 Global-scale carbon and energy flows through the marine planktonic food web: an analysis with a coupled physical–biological model Prog. Oceanogr. 120 1–28
[46] Griffies S M 2012 Elements of the Modular Ocean Model (MOM): 2012 Release (Princeton, NJ: NOAA/Geophysical Fluid Dynamics Laboratory)
[47] Large W G and Yeager S G 2009 The global climatology of an interannually varying air–sea flux data set Clim. Dyn. 33 341–64
[48] Kalnay E et al 1996 The NCEP/NCAR 40-Year Reanalysis Project Bull. Am. Meteorol. Soc. 77 437–72
[49] Danabasoglu G et al 2016 North Atlantic simulations in coordinated ocean-ice reference experiments phase II (CORE-II). Part II: inter-annual to decadal variability Ocean Model. 97 65–90
[50] Tseng Y-H et al 2016 North and equatorial Pacific Ocean circulation in the CORE-II hindcast simulations Ocean Model. 104 143–70
[51] Tittensor D P 2018 ISIMIP2a Simulation Data from Fisheries & Marine Ecosystems (Fish-MIP; global) Sector (https://doi.org/10.5880/PIK.2018.005)
[52] Walters C, Pauly D and Christensen V 1999 Ecospace: prediction of mesoscale spatial patterns in trophic relationships of exploited ecosystems, with emphasis on the impacts of marine protected areas Ecosystems 2 539–54
[53] Anticamara J A, Watson R, Gelchu A and Pauly D 2011 Global fishing effort (1950–2010): trends, gaps, and implications Fish. Res. 107 131–6
[54] Christensen V, Coll M, Buszowski J, Cheung W W L, Frölicher T, Steenbeek J, Stock C A, Watson R A and Walters C J 2015 The global ocean is an ecosystem: simulating marine life and fisheries Glob. Ecol. Biogeogr. 24 507–17
[55] Carozza D A, Bianchi D and Galbraith E D 2016 The ecological module of BOATS-1.0: a bioenergetically constrained model of marine upper trophic levels suitable for studies of fisheries and ocean biogeochemistry Geosci. Model Dev. 9 1545–65

[56] Jennings S and Collingridge K 2015 Predicting consumer biomass, size-structure, production, catch potential, responses to fishing and associated uncertainties in the world's marine ecosystems *PLoS One* **10** e0133794
[57] Dufresne J L *et al* 2013 Climate change projections using the IPSL-CM5 earth system model: from CMIP3 to CMIP5 *Clim. Dyn.* **40** 2123–65
[58] Jia F, Cai W, Wu L, Gan B, Wang G, Kucharski F, Chang P and Keenlyside N 2019 Weakening Atlantic Niño–Pacific connection under greenhouse warming *Sci. Adv.* **5** eaax4111
[59] Lotze H K *et al* 2019 Global ensemble projections reveal trophic amplification of ocean biomass declines with climate change *Proc. Natl Acad. Sci.* **116** 12907–12
[60] Bretherton C S, Widmann M, Dymnikov V P, Wallace J M and Bladé I 1999 The effective number of spatial degrees of freedom of a time-varying field *J. Clim.* **12** 1990–2009
[61] Widmann M 2005 One-dimensional CCA and SVD, and their relationship to regression maps *J. Clim.* **18** 2785–92
[62] Allen D M 1974 The relationship between variable selection and data agumentation and a method for prediction *Technometrics* **16** 125–7
[63] Dayan H, Vialard J, Izumo T and Lengaigne M 2014 Does sea surface temperature outside the tropical Pacific contribute to enhanced ENSO predictability? *Clim. Dyn.* **43** 1311–25
[64] Suárez-Moreno R and Rodríguez-Fonseca B 2015 S4CAST v2.0: sea surface temperature based statistical seasonal forecast model *Geosci. Model Dev.* **8** 3639–58
[65] Watters G M *et al* 2003 Physical forcing and the dynamics of the pelagic ecosystem in the eastern tropical Pacific: simulations with ENSO-scale and global-warming climate drivers *Can. J. Fish. Aquat. Sci.* **60** 1161–75
[66] Keenlyside N S and Latif M 2007 Understanding equatorial Atlantic interannual variability *J. Clim.* **20** 131–42
[67] Tsujino H *et al* 2020 Evaluation of global ocean–sea-ice model simulations based on the experimental protocols of the Ocean Model Intercomparison Project phase 2 (OMIP-2) *Geosci. Model Dev.* **13** 3643–708
[68] Keenlyside N S, Ding H and Latif M 2013 Potential of equatorial Atlantic variability to enhance El Niño prediction *Geophys. Res. Lett.* **40** 2278–83
[69] Bidigare R R and Ondrusek M E 1996 Spatial and temporal variability of phytoplankton pigment distributions in the central equatorial Pacific Ocean *Deep-Sea Res.* II **43** 809–33
[70] Park J-Y, Dunne J P and Stock C A 2018 Ocean Chlorophyll as a Precursor of ENSO: an earth system modeling study *Geophys. Res. Lett.* **45** 1939–47
[71] Montoya J P, Holl C M, Zehr J P, Hansen A, Villareal T A and Capone D G 2004 High rates of N_2 fixation by unicellular diazotrophs in the oligotrophic Pacific Ocean *Nature* **430** 1027–31
[72] Gruber N and Galloway J N 2008 An Earth-system perspective of the global nitrogen cycle *Nature* **451** 293–6
[73] Exarchou E, Ortega P, Rodríguez-Fonseca B, Losada T, Polo I and Prodhomme C 2021 Impact of equatorial Atlantic variability on ENSO predictive skill *Nat. Commun.* **12** 1612
[74] Cai W, Wang G, Dewitte B, Wu L, Santoso A, Takahashi K, Yang Y, Carréric A and McPhaden M J 2018 Increased variability of eastern Pacific El Niño under greenhouse warming *Nature* **564** 201–6
[75] FAO 2020 *Summary of the Impacts of the COVID-19 Pandemic on the Fisheries and Aquaculture Sector: Addendum to the State of World Fisheries and Aquaculture 2020* (Rome: FAO)